Removing Pions from Two-Nucleon Effective Field Theory

James V. Steele and R. J. Furnstahl
Department of Physics
The Ohio State University, Columbus, OH 43210
(August, 1998)

Abstract

Two-nucleon effective field theory (EFT) beyond momenta of order the pion mass is studied for both cutoff regularization and dimensional regularization with power divergence subtraction (PDS). Models with two mass scales illustrate how effects of long-distance pion physics must be removed from the coefficients that encode short-distance physics. The modified effective range expansion shows that treating pions perturbatively, as in the PDS power counting, limits the radius of convergence of the EFT. Predictions from both regularization schemes with one-pion contributions are compared to data. The breakdown of the effective field theory occurs for momenta of order 300 MeV, even using the modified effective range expansion. This behavior is shown to be consistent with that expected from two-pion contributions.

I. INTRODUCTION

Nucleon-nucleon effective field theory (NN EFT) without pions, which applies at low energies, is now well understood. Predictions are made by constructing the most general Lagrangian with nucleon fields only and fixing the coefficients by matching calculated and experimental observables in a momentum expansion. A key feature of NN EFT is the need for a nonperturbative treatment, as implied by the existence of shallow bound states such as the deuteron. Heavy propagating nucleons lead to an enhancement of loop graphs [1], which destroys the systematic power counting characteristic of perturbative EFT's [2].

Weinberg's solution was to sum certain diagrams to all orders in the loop expansion via the Schrödinger equation [1,3]. Recent analyses find this summation to be problematic for systems with large scattering lengths [4–6], which has led to alternative prescriptions within various regularization schemes [7–9]. The use of a given regularization scheme has implications on the renormalization scheme chosen because in practice calculations are truncated. The subsequent calculations of low-energy two-nucleon amplitudes have been shown to be systematic and regularization scheme independent [10,11,9], reproducing the effective range expansion of nonrelativistic potential scattering [10]. The unambiguous predictions of additional observables are in good agreement with data, as seen, for example, in the triplet state of threshold nd scattering [12], which is dominated by two-body scattering.

The characteristic breakdown scale, or radius of convergence, for a momentum expansion of the low-energy NN S-matrix is dictated by the pion. In conventional effective range theory, this breakdown is manifested by a branch point in $p \cot \delta$ at $p = m_\pi/2$ from the one-pion-exchange Yukawa potential (see Sec. II). More generally, the physical picture from effective field theory anticipates a breakdown for momenta of order $p \sim m_\pi$, as details comparable to the Compton wavelength of the pion are resolved. Predictions for external momenta above this point require taking the pion explicitly into account. In this paper, we address some of the open questions about power counting with pions and the radius of convergence of the NN EFT.

In Ref. [7], a power counting scheme was introduced, in which all pion contributions to the scattering amplitude enter perturbatively. Calculations were simplified by the use of dimensional regularization with power divergence subtraction (PDS). In contrast to Weinberg's scheme, this new approach sums only the leading contact interaction between nucleons to all orders.

Forcing a summation of higher-order contact interactions can be devastating in some regularization schemes — such as dimensional regularization with minimal subtraction — leading to undesirable systematics for a large scattering length [4,11,13]. PDS was introduced to define a consistent power counting scheme that avoids this forced summation. However, with a regularization that is solved numerically, such as cutoff regularization, it is simpler in practice to sum up these higher-order terms. We have shown previously that regularization schemes exhibiting naturalness in the bare parameters have the proper EFT behavior even when higher-order terms are summed [11]. In other words, as long as the cutoff is suitably chosen so that the theory is natural (bare parameters of order unity), the summation of higher-order terms does not affect the power counting [11], implying that cutoff regularization is an equally valid scheme for calculations.

Properly adding the pion should, in principle, increase the range in momentum for which

the EFT is predictive to the mass of particles not explicitly taken into account in the Lagrangian. Optimistic estimates in the literature anticipate a breakdown on the order of the ρ mass or $p \sim 800\,\mathrm{MeV}$ [4,8,9]. However, both dimensional [7] and cutoff [8] regularization calculations of NN scattering with pions imply a breakdown closer to $p \sim 300\,\mathrm{MeV}$. The subsequent application of EFT techniques to nuclear matter could be problematic due to the close proximity of the Fermi momentum (280 MeV) to the breakdown point.

The observed breakdown of NN EFT could have various sources. Explicit inclusion of correlated two-pion exchange, pion production, or the $\Delta(1232)$ may be necessary to increase the radius of convergence beyond several hundred MeV. The breakdown scale could even be $m_\rho/2$. However, we should first establish that the EFT is indeed limited by physics and not by how it is implemented. In the cutoff approach, simply adding one-pion exchange to the effective potential might not completely remove its influence on the radius of convergence. Qualitatively different reasons may limit the PDS approach. A renormalization group analysis [7] showed that PDS power counting should break down at a new scale $\Lambda_{\mathrm{NN}} \sim 300\,\mathrm{MeV}$, but there has been no systematic error analysis for PDS with perturbative pions.

In this paper, we address these implementation issues. Our approach generalizes the procedure of Ref. [11] by requiring the consistent removal of long-distance (pion) physics from the coefficients that encode short-distance physics. In Sec. II, we illustrate a technique to do this, called the modified effective range expansion [14], which treats pions nonperturbatively. We demonstrate its effectiveness and relevance within the context of two toy models using cutoff regularization. The modified effective range expansion is used in Sec. III to show that treating pions perturbatively within the PDS scheme limits the radius of convergence of the EFT. In Sec. IV, we compare NN scattering data to results from applying these techniques to both regularization schemes. The breakdown around $p \sim 300\,\mathrm{MeV}$ persists, but this scale is shown to be consistent with that expected from two-pion contributions. Section V is a summary of our results.

II. EXAMINING THE NEED FOR THE MODIFIED EFFECTIVE RANGE EXPANSION

The effective range (ER) expansion for nonrelativistic NN scattering [15] is derived by using analyticity arguments to relate the momentum times the cotangent of the phase shift $p\cot\delta$ to an expansion in energy $E = p^2/M$, with M the nucleon mass,[1]

$$p\cot\delta = -\frac{1}{a_s} + \frac{1}{2}\,p^2 \sum_{n=0}^{\infty} r_n \frac{p^{2n}}{\Lambda^{2n}}\,. \tag{1}$$

Here the expansion is written in terms of the lightest mass scale Λ that characterizes the underlying dynamics [7]. For example, a Yukawa or exponential potential with mass Λ limits the region of analyticity and hence validity of Eq. (1) to $p \le \Lambda/2$ [16]. Although the

[1]We restrict the discussion throughout this paper to interactions in the center of mass between two nucleons with a reduced mass $M/2$, $M = 940\,\mathrm{MeV}$, and neglect electromagnetic effects. We also take $m_\pi = 140\,\mathrm{MeV}$, $m_\rho = 770\,\mathrm{MeV}$, $f_\pi = 92\,\mathrm{MeV}$, and $\alpha_\pi = 0.075$ below.

scattering length can take on any value, we expect the ranges r_n to be of order $1/\Lambda$ [15]; this is empirically shown below. Special considerations are needed for the behavior of these ranges when the underlying potential is strong, as discussed in Sec. IV.

In our earlier work [11], we used a short-range delta-shell potential at $r = 1/m_\rho$ in the radial Schrödinger equation as a clean laboratory with which to compare various regularization schemes. As each new order in the momentum expansion of the effective potential was matched to data, we verified the improvement of the error

$$\Delta(p\cot\delta) \equiv |p\cot\delta_{\rm eff} - p\cot\delta_{\rm true}| \tag{2}$$

by powers of p^2. Contributions from different orders in the p^2 expansion become comparable at what is known as the radius of convergence of the effective field theory. We expect this to occur for momenta comparable with the underlying scale Λ. We demonstrated this by looking at error plots [8] of $\Delta(p\cot\delta)$ as a function of momentum. Both cutoff and PDS regularizations were found to give systematic behavior independent of the details of the underlying theory.

A. Delta-Shell and Exponential Model

We now add a long-range part to the underlying toy theory to model the inclusion of the pion in the analysis of NN scattering. We first study the addition of an exponential well [16] with mass m_π,

$$V(r) = -g\frac{m_\rho}{M}\,\delta(r - 1/m_\rho) - V_0\, e^{-m_\pi r}\ . \tag{3}$$

The exponential and delta-shell model the long- and short-range potentials respectively. Our ability to solve Eq. (3) analytically allows us to validate the numerical procedures used below in more realistic cases. The exponential results in singularities in $p\cot\delta$ starting at $p = -im_\pi/2$ analogous to the branch points from a Yukawa [16]. We use a "chiral-symmetry" coupling $V_0 = m_\pi^2/M$. The delta-shell coupling will be taken to be $g = 1.01$ for comparison to our earlier paper [11].

We determine the phase shift for $V(r)$ by calculating the S-wave Jost function $\mathcal{F}(p)$, which plays a key role in the modified effective range expansion [14]. This is accomplished by solving the Schrödinger equation for the Jost solution $f(p,r)$,

$$\left[\frac{d^2}{dr^2} + p^2 - MV(r)\right] f(p,r) = 0\ . \tag{4}$$

The Jost solution satisfies the asymptotic condition $f(p, r\to\infty) \to e^{ipr}$ and has the property $f(p,0) = \mathcal{F}(p)$. The exact Jost function for an exponential potential [16] can be generalized for the potential in Eq. (3) and written in terms of Bessel and gamma functions,

$$\mathcal{F}(p) = \left(\frac{y_0}{2}\right)^\nu \Gamma(1-\nu)\left[J_{-\nu}(y_0) + \frac{g\pi}{\sin\pi\nu}\frac{m_\rho}{m_\pi}J_{-\nu}(y)\left(J_\nu(y)J_{-\nu}(y_0) - J_{-\nu}(y)J_\nu(y_0)\right)\right]\ , \tag{5}$$

with $\nu = 2ip/m_\pi$, $y_0 = 2\sqrt{MV_0}/m_\pi$, and $y = y_0 e^{-m_\pi/2m_\rho}$. This satisfies the well known properties of the Jost function, namely $\mathcal{F}(p) = \mathcal{F}^*(-p^*)$ and for $V\to 0$ or $p\to\infty$, $\mathcal{F}(p)\to 1$. We can extract the exact phase shift $\delta_{\rm true}$ by using $\mathcal{F}(p) = |\mathcal{F}(p)|e^{-i\delta_{\rm true}}$.

Expressing the Bessel functions in Eq. (5) as a series, the Jost function can be expanded in powers of $1/m_\rho$,

$$\mathcal{F}(p) = \left(1 - g - g\frac{ip}{m_\rho}\right)\mathcal{J}_{-\nu}(y_0) + g\frac{y_0 m_\pi}{2m_\rho}\mathcal{J}'_{-\nu}(y_0) + \mathcal{O}\left(\frac{Q^2}{m_\rho^2}\right) , \tag{6}$$

with $Q = \{m_\pi, p\}$ and

$$\mathcal{J}_{-\nu}(y_0) \equiv \sum_{k=0}^{\infty} \frac{(-1)^k\,(y_0/2)^{2k}}{k!\,(1-\nu)\ldots(k-\nu)} . \tag{7}$$

Equation (7) shows explicitly the singularities starting at $p = -im_\pi/2$ that limit the region of analyticity of the effective range expansion. These singularities always enter multiplied by the strength of the potential y_0 and have less impact on the radius of convergence of the EFT as y_0 decreases (see below for examples).

Based on the above discussion, using a purely short-range effective potential to describe $V(r)$ should result in a breakdown at $p \sim m_\pi/2$. For S-waves, the effective potential is

$$V_{\text{eff}}(r) = C_0\delta^3(r) - \frac{1}{2}C_2\left(\overleftarrow{\nabla}^2\delta^3(r) + \delta^3(r)\overrightarrow{\nabla}^2\right) + \ldots , \tag{8}$$

which in momentum space becomes

$$V_{\text{eff}}(p,p') = C_0 + C_2\frac{p^2 + p'^2}{2} + \ldots . \tag{9}$$

It can be fixed to a given order in p by matching the C_{2n}'s to the ER parameters, Eq. (1). We do this by guessing an initial value for each of the C_{2n}'s and calculating $p\cot\delta_{\text{eff}}$. Then a fit of the difference

$$\Delta(p\cot\delta) = \alpha + \beta\,\frac{p^2}{\Lambda^2} + \ldots , \tag{10}$$

to a polynomial in p^2/Λ^2 results in the constants $\alpha, \beta, \ldots$, which are minimized up to the order of $V_{\text{eff}}(r)$ with respect to variations in the C_{2n}'s [11]. Weighting the fit by both the expected theoretical error and experimental uncertainty ensures that the EFT constants are properly obtained. The singular nature of $V_{\text{eff}}(r)$ requires regularization. We concentrate on using cutoff regularization with a cutoff Λ_c in this section, as detailed in Ref. [11]. We focus on PDS in the next section.

The cutoff Λ_c is roughly adjusted to minimize the error, which identifies the resolution scale of the underlying short-distance physics [8]. The results for using a short-distance effective potential to describe Eq. (3) are only weakly dependent on Λ_c, but are best for $\Lambda_c \sim 70\,\text{MeV}$, which are shown as the dashed lines in the left plot of Fig. 1. We plot the error $\Delta(p\cot\delta)$ as a function of momentum on a log-log plot. The lines with increasing slope refer to one, two, and three constants fixed in V_{eff} respectively. The radius of convergence can be read from the graph to be about 90 MeV. This breakdown point is directly connected to the singularity in $p\cot\delta$ at $m_\pi/2$, as can be confirmed by varying the mass in the exponential of Eq. (3).

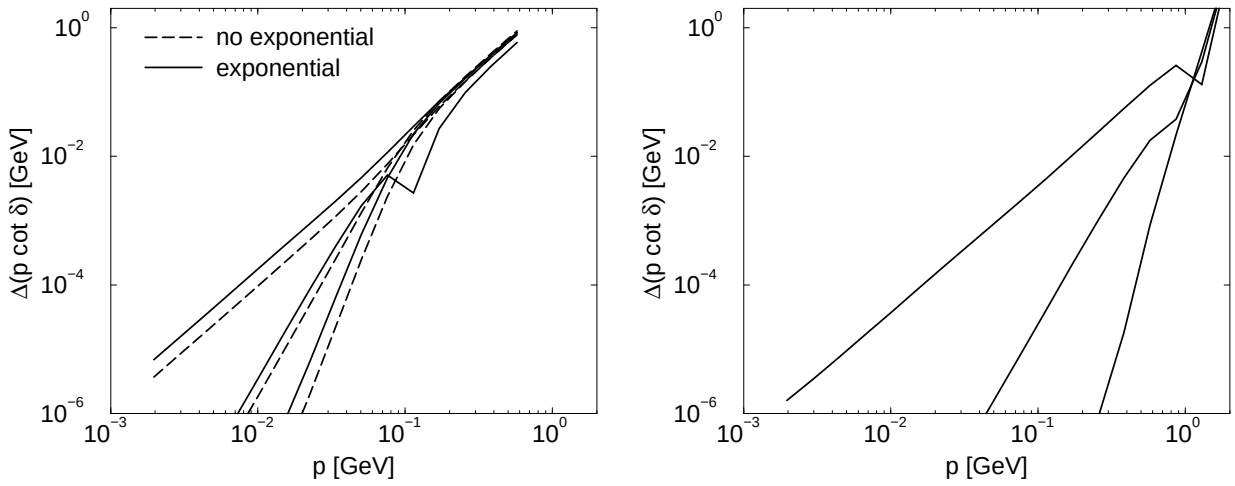

FIG. 1. The model of a delta-shell plus exponential potential, Eq. (3), with low energy constants fit by using the conventional effective range expansion (left) and modified effective range expansion (right). The radius of convergence on the left is about 90 MeV regardless of whether the exponential potential is explicitly included (solid) or not included (dashed) in the effective potential. Using the modified effective range expansion increases the radius of convergence to about 1 GeV.

It might be expected that by including the long-range behavior of the exponential potential $-V_0 e^{-m_\pi r}$ explicitly in the effective potential Eq. (8), we can increase the radius of convergence beyond $m_\pi/2$. Although the values of the C_{2n}'s from matching to the ER parameters in this case change slightly, the subsequent error plots are almost unchanged, as shown by the solid lines in the left plot of Fig. 1. *Naively taking the long-range physics into account in the cutoff effective field theory is simply not enough to yield an improved result.* A nonperturbative treatment of long-distance physics with a cutoff leads to contamination in the short-distance coefficients. This can be fixed by appropriate counterterms as discussed in Sec. III.C. But first, we show how to fix this problem using the modified ER expansion.

B. The Modified Effective Range Expansion

Properly accounting for the long-distance physics (the pion) is equivalent to removing its effects from the ER expansion. This should result in a new function with a region of analyticity larger than $p\cot\delta$ and lead to an improved radius of convergence for the EFT. After separating a general potential into a long- and short-range part $V = V_L + V_S$, such a function can be constructed and expressed in terms of the full phase shift δ and the Jost function $\mathcal{F}_L(p)$, Jost solution $f_L(p,r)$, and phase shift δ_L for the long-range potential *only* [14]:

$$K(p) = \frac{p\cot(\delta-\delta_L)}{|\mathcal{F}_L(p)|^2} + \mathrm{Re}\left[\frac{f_L'(p,0)}{\mathcal{F}_L(p)}\right] \equiv -\frac{1}{\widetilde{a}_s} + \frac{1}{2}p^2\sum_{n=0}^{\infty}\widetilde{r}_n\frac{p^{2n}}{\widetilde{\Lambda}^{2n}}\ . \tag{11}$$

The prime denotes differentiation with respect to r. Equation (11), which is called the modified effective range expansion, has been most commonly used to remove Coulomb effects from the analysis of NN scattering; it can also be generalized to higher angular momenta l [14]. The combination $K(p)$ removes the effect of the long-range potential V_L, increasing the relevant $\widetilde{\Lambda}$ to the order of the short-range potential. Thus we expect that $\widetilde{r}_n \sim 1/\widetilde{\Lambda}$. For the toy theory of Eq. (3), this would mean removing the pion singularity and moving the radius of convergence up to m_ρ, the scale of the delta-shell. Note that when the long-range potential is zero, $\delta_L = 0$, $f_L(p,r) = e^{ipr}$, and the conventional effective range expansion is recovered.

We should emphasize that the reason we introduce the modified ER expansion is to ensure that the addition of the long-range potential to our EFT does not contaminate the process of fitting the low energy constants. Once the constants are fit properly, we can return to the evaluation of the familiar observable $p\cot\delta$ to assess the improvements made by the effective field theory. When the phase shift is close to zero, $p\cot\delta$ becomes abnormally large and it can be advantageous to look at error plots of $K(p)$ instead.

We now apply the modified ER procedure to the toy model of Eq. (3). We again include the exponential $-V_0 e^{-m_\pi r}$ in the EFT, but now match the low-energy constants C_{2n} by enforcing $\Delta K(p) = 0$ to the order in p^2 we are working, similar to what was done for $\Delta(p\cot\delta)$ in Eq. (10). The exact Jost function Eq. (5) with $g = 0$ is the long-distance Jost function $\mathcal{F}_L(p)$ used in Eq. (11). Since both the EFT and the true theory have the same long-distance behavior (by construction), the term in the modified ER function that depends on $f_L'(p,0)$ cancels in the difference.

The results of the modified ER fit are shown in the right plot of Fig. 1. The optimal (natural) value of Λ_c is now about 800 MeV and the radius of convergence is seen to be about 1 GeV. Furthermore, the EFT constants that are matched using the modified ER procedure agree exactly with the values from the delta-shell potential alone [11]. This verifies that the long-distance physics is successfully removed. For more general potentials, with long- and short-distance scales of m_π and m_ρ respectively, it can be shown that the modified ER expansion Eq. (11) is the same as the pure short-distance ER expansion up to terms of $\mathcal{O}(m_\pi^2/m_\rho^2)$ [17]. These corrections are actually zero for a delta-shell potential.

When comparing to data, we expect to have some error in the long-range potential used in our effective theory compared to the underlying theory. We can estimate the effect this will have on our results by purposely detuning the value of V_0 used in the long-range part of our effective potential. The fit to three constants is sensitive enough to fail if the error is larger than a fraction of a percent. The fit to one constant gives consistent results regardless of the error. The comparison of the results for a fit to two constants is shown in Fig. 2 for errors of 5, 10, and 50 percent. Although the results are not as clean as in the error-free case, we can read off a radius of convergence by taking a straight line from the low energy behavior. This shows that the radius of convergence inferred from the plot slowly reduces as the error in V_0 increases. As long as the discrepancy in the long-range part of the effective field theory and that from data do not differ by more than 5%, the results for one and two constants are fairly stable.

Using the modified ER expansion is a guaranteed way to properly incorporate the long-distance physics in the EFT. However, at least some improvement in the radius of convergence was found in the case of NN scattering without this technique [3,8]. We use a

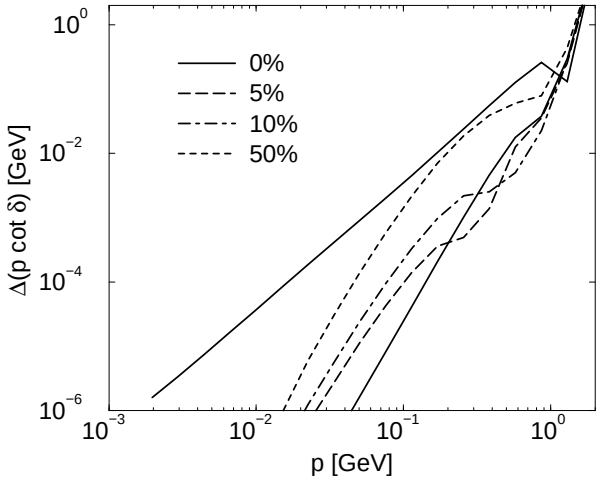

FIG. 2. The dependence of the two-constant fit to Eq. (3) on the percentage error in V_0.

second model in the next subsection to further investigate when the modified ER expansion is needed.

C. Two-Yukawa Model

A more representative toy model of nuclear forces consists of two Yukawas of masses m_π and m_ρ. We require

$$V(r) \stackrel{r\to\infty}{\longrightarrow} -\alpha_\rho \frac{e^{-m_\rho r}}{r} - \alpha_\pi \frac{e^{-m_\pi r}}{r}\,, \tag{12}$$

but for small r the results are practically independent of whether a cut-off Yukawa [8] or a hard core repulsion are used to regulate the potential at the origin. For simplicity, we take Eq. (12) as the exact potential and merely exclude the origin. The couplings are initially taken to be $\alpha_\pi = 0.075$, as given by one-pion exchange in ${}^1S_0$ NN scattering, and $\alpha_\rho = 1.05$, which gives the large scattering length found in that channel, $a_s = -25\,\mathrm{fm}$. Equation (12) models the short-distance physics with a single scale. Nuclear phenomenology suggests that the short-range Yukawa actually should be replaced by the combination of attractive and repulsive Yukawas resulting from the exchange of scalar and vector mesons [18]. We will come back to this issue in Sec. IV.

Since the long-distance physics is dictated by the pion, the effective Lagrangian that describes this model problem is identical to that for NN scattering [1,7]

$$\begin{aligned}\mathcal{L}_{\rm eff} = N^\dagger \left[i\partial_t + \frac{\nabla^2}{2M} - \frac{g_A}{2f_\pi}\sigma\cdot\nabla(\pi\cdot\tau)\right] N \\ -C_0(N^\dagger N)^2 + \frac{1}{2}C_2\left[(N^\dagger\nabla N)^2 + ((\nabla N^\dagger)N)^2\right] + \dots\,,\end{aligned} \tag{13}$$

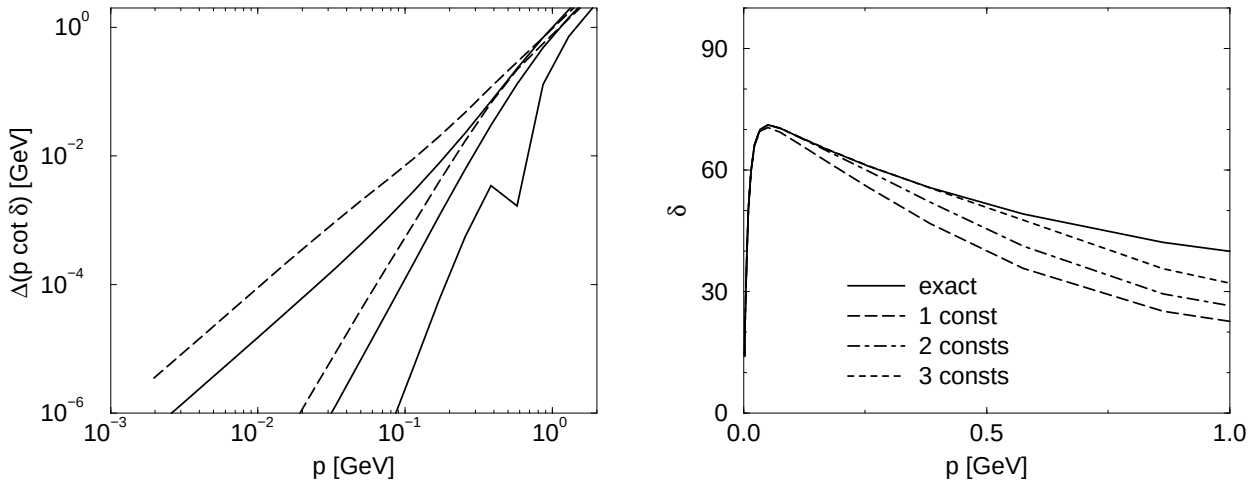

FIG. 3. The error in $p \cot \delta$ (left) and the phase shift in degrees (right) for the two-Yukawa toy model. The solid curves on the left show errors from the modified ER fit to one, two, or three constants, which are independent of the strength of V_L. Without using the modified ER procedure, similar results are obtained for one and two constants with a weak α_π. The dashed curves on the left show the errors as well as the radius of convergence worsen if α_π is made a factor of three stronger.

with the ellipses representing terms with more than one pion field as well as higher-derivative terms. Neglecting retardation effects since they are absent from the underlying toy model by construction, Eq. (13) can be expressed in terms of a potential (for the ${}^1S_0$ channel)

$$V_{\rm eff}(r) = -\alpha_\pi \frac{e^{-m_\pi r}}{r} + \left(C_0 + \frac{4\pi\alpha_\pi}{m_\pi^2} \right) \delta^3(r) - \frac{1}{2} C_2 \left(\overleftarrow{\nabla}^2 \delta^3(r) + \delta^3(r) \overrightarrow{\nabla}^2 \right) + \dots \ , \qquad (14)$$

with $\alpha_\pi = g_A^2 m_\pi^2 / 16\pi f_\pi^2$, showing that the long-distance physics of the pion from Eq. (12) is included exactly. The full effective potential, including the pion Yukawa, is regularized at short distances by a cutoff Λ_c [8].

The Jost functions for both the full phase shift and the long-distance part required in Eq. (11) are calculated numerically, as outlined in Appendix A. Note that when calculating the modified ER expansion $K(p)$, we still impose a cutoff on the potential Eq. (12), as would be done if the underlying potential were not exactly known.

The results from using the modified ER expansion to fit one, two, and three constants are shown by the solid lines in the left plot of Fig. 3 for the optimal value $\Lambda_c = 600\,\text{MeV}$. The phase shifts themselves are shown in the right plot. While the improvement in the phase shifts is manifest, it is clear that the error plots are needed to make a quantitative assessment of the convergence. The plots show the radius of convergence is between 500 and 600 MeV, which is comparable to the range of analyticity $m_\rho/2$ of the modified ER expansion. For comparison, we also used a delta-shell at $r = 1/m_\rho$ as the short-distance potential (see Appendix A). This gives a radius of convergence of about 1 GeV, which is in agreement with the exponential potential model in the previous subsection, and shows the different impact from branch point and pole singularities in $p \cot \delta$.

TABLE I. Conventional and modified effective range parameters for the two-Yukawa model. The pion Yukawa was cut off at $p = 500\,\mathrm{MeV}$ to calculate the modified ER function. In parentheses the ranges are expressed in terms of corresponding powers of the expected underlying scale.

	a_s (fm)	r_0 (fm)	r_1/Λ^2 (fm^3)	r_2/Λ^4 (fm^5)
ER	-25.1	1.63 $(1.2/m_\pi)$	-3.4 $(-1.2/m_\pi^3)$	16. $(2.9/m_\pi^5)$
Mod. ER	-1.72	0.667 $(2.6/m_\rho)$	-0.024 $(-1.4/m_\rho^3)$	0.0028 $(2.6/m_\rho^5)$

The first few ER parameters from $p\cot\delta$ in Eq. (1) are given in Table I. As anticipated, the ranges are all on the order of $1/m_\pi$. The modified ER expansion leads to values more naturally expressed in powers of $1/m_\rho$. Once again we find that the modified ER parameters truly have the long-distance physics removed, allowing for a clean fit to our EFT and resulting in an improved radius of convergence. Introducing some error into the value of α_π, as studied in the last subsection, leads not only to an inability to fit three constants but also to unnatural modified ER parameters. This effect may provide a way to work towards a more accurate value for α_π.

Using the conventional ER expansion to fit one or two constants in the EFT, though, gives results just as good as from using the modified ER expansion. It only fails at three constants. Since $\alpha_\pi \sim m_\pi/m_N$ is weak, the importance of the long-distance potential, as well as the need for the modified ER expansion, are reduced. The same result occurs in the model of the exponential well if the strength of the potential is decreased. This behavior will be explained in the next section. Regardless, the robustness of the fit to the ER parameters for the two approaches is not qualitatively the same. The success of the conventional ER fit depends strongly on the initial guess for the EFT constants and the weighting of the fit in Eq. (10) by the theoretical error. These hindrances, which do not play a major role in the modified ER procedure, could make it difficult to fit to real data with experimental uncertainties.

By increasing α_π, we should see the radius of convergence from using the conventional ER fit decrease while the modified ER result is unchanged. This is illustrated by the dashed lines in the left plot of Fig. 3, which show results for the conventional ER fit after enhancing α_π by a factor of three. The radius of convergence is only about 300 MeV for the optimal $\Lambda_c = 400\,\mathrm{MeV}$. The results from using the modified ER procedure are insensitive to the strength of the long-range coupling constant.

In summary, for a basic two-scale problem, the modified ER procedure provides a systematic removal of the long-distance physics, which ensures a proper, robust fit to the low-energy constants, even with a strong long-range potential. This often results in a better radius of convergence for our EFT, although the improvement is not significant for a weak long-range potential. In addition, the modified ER parameters $\widetilde{r}_n$ from Eq. (11) are all on the order of the range of the short-distance potential, $1/m_\rho$.

III. ARE NONPERTURBATIVE PIONS NEEDED?

We now turn to the PDS regularization scheme introduced in Ref. [7], which used the language of Feynman diagrams. The nonrelativistic Lagrangian of Eq. (13) gives the pion-

nucleon vertex

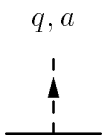

$$= \frac{g_A}{2f_\pi}\tau^a\,\sigma\cdot q\,, \tag{15}$$

and so, after projection onto the ${}^1S_0$ partial wave, one-pion exchange contributes ($q = p - p'$)

$$\frac{g_A^2}{4f_\pi^2}\left[-1 + \frac{m_\pi^2}{4p^2}\,\ln\!\left(1 + \frac{4p^2}{m_\pi^2}\right)\right] \tag{16}$$

to the full amplitude

$$\mathcal{A} = \frac{4\pi}{M}\frac{e^{2i\delta}-1}{2ip} = \frac{4\pi}{M}\frac{1}{p\cot\delta - ip}\,. \tag{17}$$

Notice that the amplitude develops a branch point in momentum at $p = -im_\pi/2$ when the pion Eq. (16) is included, as expected from the effective range expansion.

The loop integrals are evaluated in dimensional regularization with the PDS scheme, which subtracts all poles coming from four or fewer dimensions [7]. For example, the one-loop bubble diagram of two nucleons with external momentum $p = \sqrt{ME}$ becomes

$$-i\left(\frac{\mu}{2}\right)^{4-D}\int\frac{d^Dq}{(2\pi)^D}\,\frac{i}{E/2 + q_0 - \mathbf{q}^2/2M + i\epsilon}\,\frac{i}{E/2 - q_0 - \mathbf{q}^2/2M + i\epsilon} = -\frac{M}{4\pi}(\mu + ip)\,. \tag{18}$$

An arbitrary mass scale μ is introduced to ensure that coupling constants multiplying the integral Eq. (18) retain their dimension when D is taken different from four. Physical quantities are independent of μ, which has two consequences: (i) the coupling constants C_{2n} in Eq. (13) must depend on μ to cancel the μ-dependence of the loop integrals; and (ii) μ must be of the same order as p or smaller to ensure that the integral Eq. (18) is properly counted in a momentum expansion.

A. PDS Renormalization Group

The PDS power counting requires the constants in the effective Lagrangian scale like $C_0 \sim 1/\mu$ and $C_2 \sim 1/\mu^2$ when considering momenta $p \sim \mu \gg 1/a_s$ [7]. This is particularly relevant for S-wave NN scattering, where the scattering length is large. Furthermore, one-pion exchange scales like $\mathcal{O}(p^0)$ as in Eq. (16) and nucleon loops scale like $\mathcal{O}(p)$ as in Eq. (18). Therefore, every n–loop diagram with insertions of the contact term C_0 scales like $\mathcal{O}(p^{-1})$. To have a consistent power counting, they must be summed [7], producing the leading-order amplitude depicted in Fig. 4,

$$\mathcal{A}_{-1} = -\frac{C_0}{1 + C_0\frac{M}{4\pi}(\mu + ip)}\,. \tag{19}$$

Matching $\mathcal{A}_{-1}$ to the leading-order effective range expansion then determines the μ dependence of C_0,

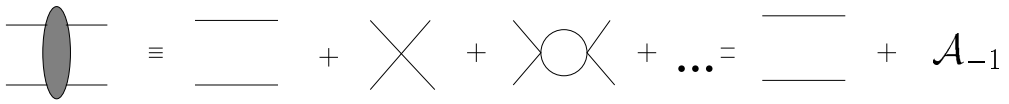

FIG. 4. Leading order diagrams in the PDS power counting with C_0 at each vertex.

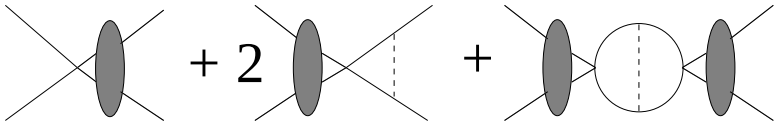

FIG. 5. All μ-dependent diagrams that contribute to the β-function for C_0 to order $\mathcal{O}(p^0)$.

$$C_0(\mu) = \frac{4\pi}{M}\left(\frac{1}{-\mu + 1/a_s}\right) + \mathcal{O}(\mu^0)\ , \tag{20}$$

confirming the scaling $C_0 \sim 1/\mu$.

At subleading order $\mathcal{O}(p^0)$, perturbative corrections from one-pion exchange and C_2 insertions begin to contribute. For non-zero pion mass, a term of the form $D_2\, m_\pi^2$ also enters. Since to this order only the combination $C_0 + m_\pi^2 D_2$ appears, we absorb D_2 into the definition of C_0 for convenience. Matching the amplitude to this order in the effective range expansion

$$p\cot\delta = ip + \frac{4\pi}{M\mathcal{A}_{-1}} - \frac{4\pi\mathcal{A}_0}{M\mathcal{A}_{-1}^2} + \cdots \tag{21}$$

determines the μ-dependence of the low-energy constants. Using the explicit expression for the subleading amplitude $\mathcal{A}_0$ in Ref. [7], we obtain

$$C_0(\mu) = \frac{4\pi}{M}\left(\frac{1 + 2(\mu - m_\pi)/\Lambda_{\rm NN}}{-\mu_\pi + 1/a_s}\right) + \mathcal{O}(\mu) \tag{22}$$

$$C_2(\mu) = \frac{MC_0^2}{8\pi}\Bigg[r_0 - \frac{g_A^2 M}{24\pi f_\pi^2}\Bigg(3 - 8\frac{\mu}{m_\pi} + 6\frac{\mu^2}{m_\pi^2} + \frac{16\pi}{Mm_\pi C_0}\left(3\frac{\mu}{m_\pi} - 2\right) + \frac{96\pi^2}{(Mm_\pi C_0)^2}\Bigg)\Bigg] + \mathcal{O}(\mu)\,, \tag{23}$$

where

$$\mu_\pi \equiv \mu + \alpha_\pi M \ln\frac{\mu}{m_\pi} + \frac{(\mu - m_\pi)^2}{\Lambda_{\rm NN}}\,, \tag{24}$$

and $\Lambda_{\rm NN} = 16\pi f_\pi^2/g_A^2 M \simeq 300\,\text{MeV}$. At $\mu = m_\pi$, these expressions reproduce the matching condition quoted in Ref. [7]. The expression for C_0 also coincides with the leading order result Eq. (20) for this choice of μ.

Solving the renormalization group equation for C_0 is another way to generate its μ dependence. A calculation order-by-order in the number of loops is not equivalent to solving it in powers of momentum due to the nonperturbative nature of the power counting. Expanding

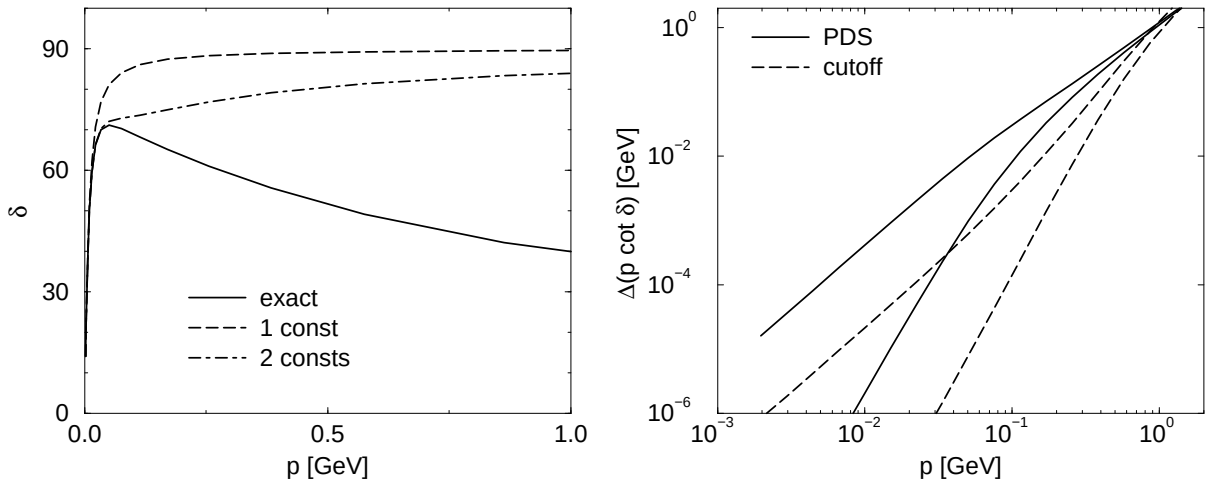

FIG. 6. The left plot shows the exact phase shift in degrees for the two-Yukawa model and the results from one (dashed) and two (dot-dashed) constants in PDS with $\mu = m_\pi$. The right side shows the error in $p \cot \delta$ for these cases (solid) as well as for the cutoff regularization (dashed) of Fig. 3.

the amplitude, which is an observable, in powers of momentum requires that the sum of all graphs to a given order is μ-independent. At subleading order, the μ-dependent graphs are shown in Fig. 5, and applying $\mu\frac{\partial}{\partial\mu}$ to their explicit expressions from Ref. [7] results in the renormalization group equation

$$\mu\frac{\partial C_0}{\partial\mu} = \frac{M\mu}{4\pi}\left[C_0^2 + \left(\frac{\alpha_\pi M}{\mu}C_0^2 + \frac{g_A^2}{2f_\pi^2}C_0\right)\frac{1}{1+2(\mu-m_\pi)/\Lambda_{\rm NN}}\right] + \mathcal{O}(\mu)\,, \tag{25}$$

whose solution is the expression Eq. (22), already obtained from matching. The solution is consistent with the power counting for all μ, behaving like $C_0 \sim 1/\mu$. This is in contrast to a renormalization group analysis based on a loop expansion, whose solution is inconsistent with the power counting for $\mu \gtrsim \Lambda_{\rm NN}$ [7]. Although the above discussion was just for the ${}^1S_0$ channel, the results also hold for the ${}^3S_1$ channel since the pion contribution is identical in the two cases to this order.

B. PDS and the Modified Effective Range Expansion

We can now apply the relations Eq. (20)–(23) to generate the leading and subleading behavior of PDS. The error plots for the two-Yukawa model from Sec. II.C using PDS are compared in Fig. 6 with the cutoff results. Matching the constants to data ensures μ-independent observables only to the order they were fixed; the remaining error still depends on the choice of μ. This is different from the case with a short-range potential only [11], since pions contain μ-dependent terms to all orders in the momentum expansion. However, the results are relatively stable for $\mu \leq 450\,\text{MeV}$. The radius of convergence (from extrapolating the slopes at small p) is about $p \simeq m_\pi$, which is much smaller than from cutoff regulariza-

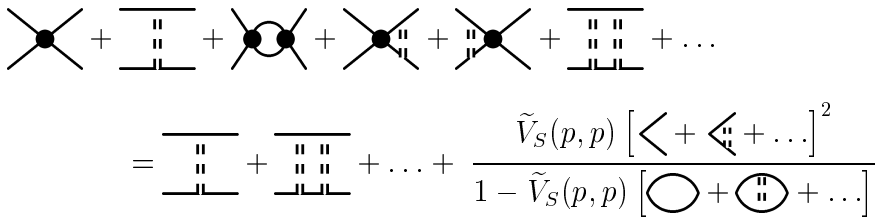

FIG. 7. A Feynman-diagram identity for the Lippmann-Schwinger equation in dimensional regularization.

tion.[2] In fact, using a purely short-range effective potential with cutoff regularization gives almost the same results as PDS with pions.

This implies the pion is not being properly taken into account, as can be seen in the power counting of C_2. Without pions, the scaling is $C_2 \sim 1/\mu^2$, but Equation (23) shows the pion contributions begin to dominate for $\mu \sim m_\pi$, leading to

$$C_2(\mu > m_\pi) \sim -\frac{8\pi\alpha_\pi}{m_\pi^2}\,. \tag{26}$$

The power counting for $C_2 p^2$ therefore breaks down for momenta above m_π. A nonperturbative treatment of pions might remedy this situation. It is instructive, therefore, to investigate how the PDS power counting differs from the modified ER expansion, which was so successful in the previous section.

First, we show that, for dimensional regularization, solving the Schrödinger equation with the potential Eq. (14) is the same as using the modified ER expansion. This can be shown diagrammatically for the truncated potential $V_S(p,q) = C_0 + C_2(p^2+q^2)/2$. The amplitude $\mathcal{A}$ is found by solving the Lippmann-Schwinger equation, which is equivalent to solving the Schrödinger equation. In dimensional regularization, factoring the potential out of the loop integrals produces an additional contribution to the potential $\delta V_S(p,p) = -\alpha_\pi m_\pi M C_2$, leading to $\widetilde{V}_S = V_S + \delta V_S$. Denoting the long-range pion Yukawa[3] (V_L) with a double dashed line and the short-range delta-function terms (V_S) by a dot, the amplitude $\mathcal{A}$ can then be shown to satisfy the Feynman-diagram identity [4] in Fig. 7.

The first group of terms on the right-hand side of Fig. 7 is just the one-pion exchange amplitude $\mathcal{A}_L$, which in turn is related to the long-range phase shift δ_L by an expression

---

[2] There is a narrow window around $\mu = 400\,\mathrm{MeV}$ in which the radius of convergence increases to about 300 MeV. Fine-tuning μ gives results qualitatively similar to fine-tuning D_2 as a third parameter as done in Ref. [7]. In that fit, however, the accuracy in the determination of the ER parameters a_s and r_e was sacrificed in order to minimize global errors for $p \le 200\,\mathrm{MeV}$. In contrast, Eqs. (22)–(23) can be used to fine-tune μ while still observing the matching requirements, leading to proper error plots and systematic results. We will not exploit this effect but instead take $\mu = m_\pi$ as in Ref. [7].

[3] Note from Eq. (14) that part of the pion contribution is proportional to a delta-function and is therefore absorbed in V_S.

analogous to Eq. (17). The coefficient of $\widetilde{V}_S$ in the denominator of the last term is the Green's function (see Appendix B)

$$G_E(r=0,r'=0) = \langle 0|\frac{1}{E-H_L+i\epsilon}|0\rangle = -\frac{M}{4\pi r}\frac{f_L(p,r)}{\mathcal{F}_L(p)}\bigg|_{r=0}, \tag{27}$$

and the coefficient of $\widetilde{V}_S$ in the numerator is given by the square of [4]

$$\int \frac{d^3q}{(2\pi)^3}\langle q|(1+G_E V_L)|p\rangle = \frac{1}{\mathcal{F}_L(p)}\,. \tag{28}$$

Therefore the diagrammatic identity can be rewritten as

$$\frac{4\pi}{M}\frac{|\mathcal{F}_L(p)|^2}{p\cot(\delta-\delta_L)-ip} = -\frac{\widetilde{V}_S(p,p)}{1-\widetilde{V}_S(p,p)G_E(0,0)}\,. \tag{29}$$

Calculating $G_E(0,0)$ in the PDS scheme with nonperturbative pions (see Appendix B) leads to the modified ER function Eq. (11),

$$\begin{aligned} K^{\rm PDS}(p) &= -\frac{4\pi}{M\,\widetilde{V}_S(p,p)} - \mu - \alpha_\pi M \ln\frac{\mu}{m_\pi} - c_\pi \\ &= -\frac{1}{\widetilde{a}_s} + \frac{1}{2}\widetilde{r}_0 p^2 + \dots\,, \end{aligned} \tag{30}$$

where c_π and therefore $\widetilde{a}_s$ are both regularization scheme dependent. Matching the first two terms in the p^2 expansion gives

$$\widetilde{C}_0(\mu) = -\frac{4\pi}{M\mathcal{D}} + \alpha_\pi m_\pi \frac{2\pi\widetilde{r}_0}{\mathcal{D}^2} \tag{31}$$

$$\widetilde{C}_2(\mu) = \frac{2\pi\widetilde{r}_0}{M\mathcal{D}^2} \tag{32}$$

$$\mathcal{D} = \mu + \alpha_\pi M \ln\frac{\mu}{m_\pi} - \left(\frac{1}{\widetilde{a}_s} - c_\pi\right)$$

where $\widetilde{C}_0$ includes the short-distance pion contribution [see Eq. (14)]. These expressions are very different from the perturbative pion results Eq. (22-23) and lead to

$$\widetilde{C}_2(\mu) \sim \frac{2\pi\widetilde{r}_0}{M}\frac{1}{\mu^2}\,, \tag{33}$$

which does not exhibit a breakdown in the scaling.

Removing the effect of the pions nonperturbatively, as in the above modified ER procedure, leaves only a residual short-range potential. PDS reproduces the modified ER expansion by construction in this case, with μ-independent results just as for a purely short-range potential [11]. The error plots for the two-Yukawa model, shown in Fig. 8, illustrate the improvement of the PDS radius of convergence from about 150 MeV with perturbative pions to about 800 MeV with nonperturbative pions.

Taking pions into account perturbatively, as in the original PDS power counting scheme, leads to a breakdown in the scaling of the EFT constants. This is reflected by the radius of

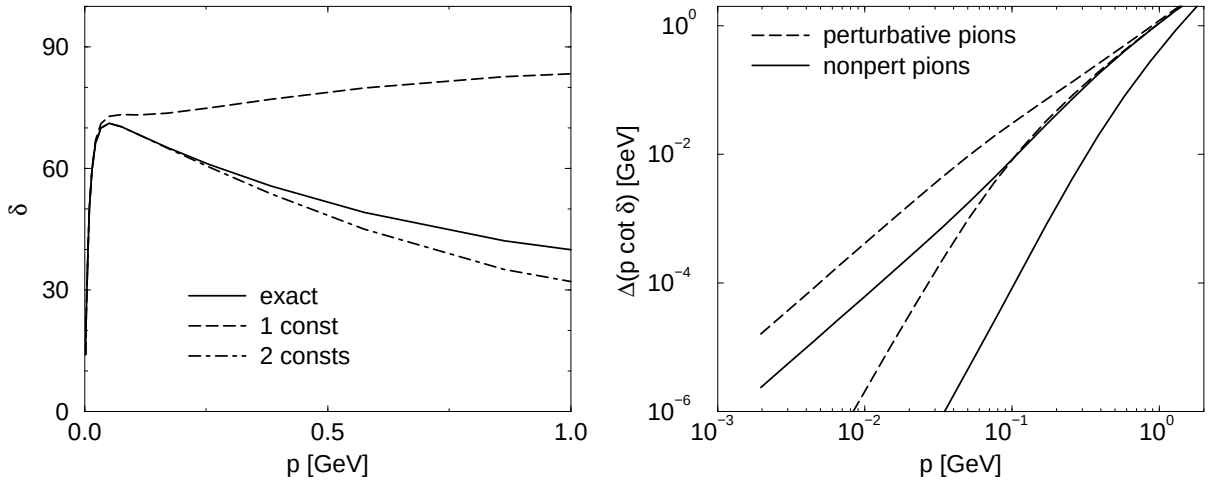

FIG. 8. The left plot shows the exact phase shift in degrees for the two-Yukawa model and the results from one (dashed) and two (dot-dashed) constants in PDS with nonperturbative pions. The right side shows the error in $p \cot \delta$ for these cases (solid) as well as for the perturbative pion case (dashed) of Fig. 6.

convergence still set by m_π as in Fig. 6. Implementing nonperturbative pions, either through using the modified ER expansion or solving the Schrödinger equation, rectifies the situation, leading to an improved radius of convergence set by the next scale in the underlying theory. It is not clear if some modification of the perturbative pion counting scheme can be devised to transcend this problem. For example, a global fitting procedure that does not enforce an exact match of the low energy data could lead to a better overall error [7] in Fig. 8. However, the ability to determine a radius of convergence graphically is lost in this case, requiring further analysis to determine the breakdown scale.

C. Cutoff Regularization and the Modified Effective Range Expansion

We return to cutoff regularization within the context of the above arguments. In this case, the potential V_S cannot be factored out of the loop integrals in Fig. 7, so the Schrödinger equation and modified ER expansion are not as simply related. In particular, the finite cutoff generates additional terms on the right-hand-side of Fig. 7 that contribute to the contact interactions. For example,

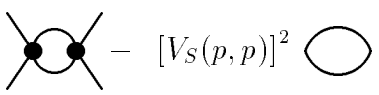

$$[V_S(p,p)]^2 \sim -\frac{M\Lambda_c^3}{6\pi^2}\Big(C_0 + \frac{4\pi\alpha_\pi}{m_\pi^2}\Big)C_2 + \dots\,, \tag{34}$$

which can be interpreted as a shift of the short-range potential V_S in the modified ER expansion. The combination in parentheses originates from Eq. (14). It was shown in Ref. [11] that an unnatural cutoff leads to an unnaturally large C_0, reducing the radius of

TABLE II. Conventional and modified effective range parameters for S-wave np scattering. The pion Yukawa was cut off at $p = m_\rho/2$. All numbers are in appropriate powers of fm. In parentheses the ranges are expressed in terms of possible underlying scales, with $m_\sigma = 500\,\mathrm{MeV}$.

		a_s (fm)	r_0 (fm)	r_1/Λ^2 (fm^3)	r_2/Λ^4 (fm^5)
$^1S_0$	ER	-23.4	2.63 $(1.9/m_\pi)$	-0.25 $(-0.091/m_\pi^3)$	1.7 $(0.31/m_\pi^5)$
	Mod. ER	-1.70	3.10 $(7.9/m_\sigma)$	1.5 $(24./m_\sigma^3)$	-0.53 $(-55./m_\sigma^5)$
$^3S_1$	ER	5.39	1.75 $(1.2/m_\pi)$	0.21 $(0.074/m_\pi^3)$	0.16 $(0.030/m_\pi^5)$
	Mod. ER	-7.46	2.12 $(5.4/m_\sigma)$	0.32 $(5.2/m_\sigma^3)$	0.28 $(29./m_\sigma^5)$

convergence of the EFT. Thus an analogous effect should follow if α_π is large. This is why a strong long-range potential such as in the exponential and delta-shell model of Sec. II.A has better results in cutoff regularization from using the modified ER expansion as opposed to the Schrödinger equation. However, a weak coupling, as occurs in NN scattering, leads to almost no difference in the radius of convergence.

IV. APPLICATION TO DATA

Now that we have a better understanding of what sets the breakdown scale for the EFT, we can apply the techniques of the previous sections to the problem of NN scattering. We take our data from the Nijmegen partial wave analysis [19], since it gives the most stable results over a large momentum range. As we saw in the two-Yukawa model of Sec. II.C, the ER and modified ER parameters reflect the corresponding scales of the underlying physics quite nicely. Table II makes the same comparison using the np scattering S-waves.[4] Note that the mass scale needed to make the modified ranges $\widetilde{r}_n$ of order unity is actually *smaller* than the ranges r_n, in stark contrast to the clean systematics of the two-Yukawa model.

This difference can also be seen in the error plots for the $^1S_0$ partial wave in Fig. 9. As anticipated by the two-Yukawa model, the modified ER and conventional ER results for cutoff regularization give identical results, due to the weak coupling of the pion. However, the optimal cutoff is $\Lambda_c = 250\,\mathrm{MeV}$ with a resulting radius of convergence of about 300 MeV, consistent with the analysis of Ref. [8]. This is much lower than the 500-600 MeV radius of convergence of the two-Yukawa model. The PDS results for $\mu = m_\pi$ (left plot of Fig. 9) break down earlier than cutoff regularization with a worse absolute error, although μ can again be tuned to improve the PDS error plots (as in Sec. II.C). Using PDS with nonperturbative pions improves the radius of convergence (right plot of Fig. 9), leading to results comparable with the cutoff, as also seen in the last section.

The fact that the modified effective ranges and the radius of convergence reflect a smaller scale than 500 MeV must be due to a feature of the data that our two-Yukawa model did not simulate. Retardation and relativistic effects are not included in the model, but at these energies they are small and should be negligible. In the np system, electromagnetic effects

[4]The precise values in Table II are somewhat sensitive to our choice of data and fitting procedure.

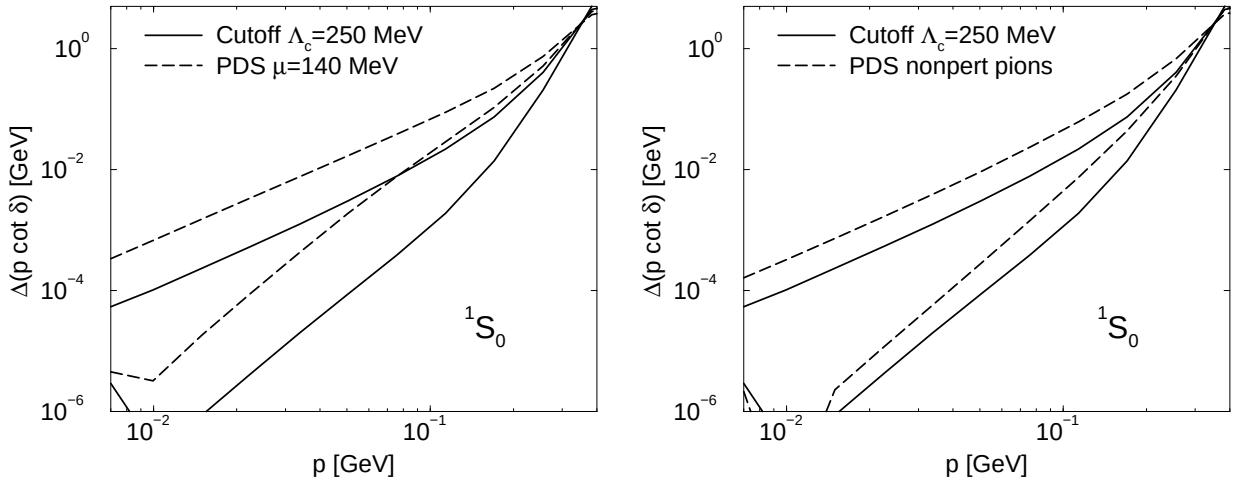

FIG. 9. The ${}^1S_0$ np error in $p\cot\delta$ for cutoff regularization with $\Lambda_c = 250\,\mathrm{MeV}$ (solid) and for PDS (dashed), both shown for one and two constants. The PDS results are for $\mu = m_\pi$ and perturbative pions in the left plot and for nonperturbative pions in the right plot.

are very small in phenomenological models that parameterize the data [19,20]. Details of the hadronic structure are only expected to appear for momenta above 500 MeV [8]. Errors in the value of α_π or in the data have some effect on the values of the higher-order range parameters, but do not appreciably change the ranges quoted in Table II or the error plot of Fig. 9.

There are two features which are not as easy to rule out: the pion-production inelastic threshold, at about $p \simeq 360\,\mathrm{MeV}$, and correlated two-pion exchange, which gains strength above $p \simeq 400\,\mathrm{MeV}$, both of which are close to the breakdown scale in Fig. 9. Conventionally, the latter effect has been modeled using a σ meson with a mass of about 500 MeV [18]. Naive dimensional analysis shows that two-pion effects are the same order as the C_2 contact term, and could prove to be important [8]. This would imply a breakdown at about $m_\sigma/2 \sim 250\,\mathrm{MeV}$ and modified effective ranges with behavior $\widetilde{r}_n \sim 1/m_\sigma$. The error plots of the data (Fig. 9) are consistent with this effect, but the ranges, as shown in Table II, are not.

We can test the dependence of our analysis on two-pion contributions by replacing the single short-distance Yukawa in the two-Yukawa model by two short-distance Yukawas representing an attractive σ meson of mass 500 MeV and a repulsive vector meson (normally associated with both the ω and ρ mesons, but we will generically label it with a ρ):

$$V(r) \stackrel{r\to\infty}{\longrightarrow} \alpha_\rho \frac{e^{-m_\rho r}}{r} - \alpha_\sigma \frac{e^{-m_\sigma r}}{r} - \alpha_\pi \frac{e^{-m_\pi r}}{r}\,. \tag{35}$$

Our two-Yukawa model Eq. (12) averaged the two short-distance effects into a single (attractive) short-ranged Yukawa for simplicity. Choosing an arbitrary value for α_σ, we tune α_ρ to obtain the large scattering length of NN scattering S-waves. We consider two representative solutions: one with weak couplings $(\alpha_\sigma, \alpha_\rho) = (1.5, 1.5)$ and one with strong couplings $(\alpha_\sigma, \alpha_\rho) = (7, 14.65)$. The strong couplings are similar to couplings used in the Bonn poten-

tial to describe NN scattering [18] and are the size expected from naive dimensional analysis [21].

When the weak couplings are used, the modified ER approach provides a clean removal of the short-distance physics in both the error plots and the $\widetilde{r}_n$'s, similar to what was seen for the two-Yukawa model in Sec. II.C. Applying the same procedure to the strong coupling solution, however, gives remarkably similar results to those found with the data. In particular, the effective ranges behave similarly to those in Table II, with the underlying scale for the modified effective ranges seemingly worse than the conventional effective ranges, and the radius of convergence drops from 600 MeV to 300 MeV in the error plots. In our model, we can explicitly prove that the breakdown is associated with $m_\sigma/2$ (and not $2m_\pi$ for example) by increasing the scalar mass. As m_σ increases to m_ρ, the results smoothly shift to those of the two-Yukawa model.

Therefore, the pion is successfully removed by the modified ER expansion, leaving the next scale $m_\sigma/2$ to set the radius of convergence. Just as a weak pion did not require the modified ER expansion for an improved radius of convergence, a weak scalar coupling α_σ does not affect the breakdown. This explains why only the strong coupling solution fails at $m_\sigma/2$. A strong coupling also means the range of the interaction is not $\mathcal{O}(1) \times 1/m_\sigma$ [18]. The dimensionless strength of the potential is $\eta_\sigma \equiv \alpha_\sigma M/m_\sigma \sim 13$. Investigation of the three-Yukawa model Eq. (35) indicates that the modified effective ranges should scale as $\widetilde{r}_n \sim \eta_\sigma^n/m_\sigma$. The results in Table II are indeed consistent with this scaling.

Thus the large modified effective ranges in NN scattering $\widetilde{r}_n$ imply that two-pion contributions are strong. If this is so, these two-pion effects should be included in the modified ER procedure as long-distance physics in order to go beyond $p \sim 300$ MeV. It is straightforward to test this conclusion in the three-Yukawa model by including the σ in the long-distance potential. As expected, this leads to an improved radius of convergence. The next step should be to use the explicit form for the two-pion physics in an EFT analysis of data with the modified ER procedure.

V. SUMMARY

An effective field theory (EFT) approach to low-energy QCD systematically treats the physics of different length scales. For applications to nonrelativistic NN scattering and nuclear structure, distance scales corresponding to momenta up to several times the pion mass may be relevant. In this regime, the long-distance physics is dictated by the pion through chiral symmetry. The short-distance physics is replaced by a generic expansion in powers of the momentum over a scale determined by the remaining underlying interactions. This conceptually simple procedure promises a systematic description of two-nucleon processes.

The nonperturbative nature of nuclear forces complicates this EFT approach, leading to open questions about including pions within various regularization and power counting schemes. In this paper, we have examined cutoff regularization and dimensional regularization with the PDS scheme. Toy models were used to analyze both approaches in a controlled fashion before confronting NN scattering data. We find that the implementation of these schemes can be subtle.

Within cutoff regularization, simply adding a one-pion-exchange potential to a short-range effective potential does not necessarily improve the radius of convergence of the EFT.

This is because the cutoff mixes long-distance contributions with the short-distance constants, which can lead to unnaturally large corrections. Only if the long-distance coupling is weak, as occurs for one-pion exchange in NN scattering, are these extra contributions negligible. By using the modified effective range (ER) procedure, however, a consistent removal of the long-distance physics can be implemented for all strengths of the interaction.

In the PDS scheme, the long-distance pion physics is accounted for perturbatively with a consistent power counting prescription. A systematic error analysis of a two-scale model showed, however, that an EFT with the PDS power counting breaks down earlier than cutoff regularization. This breakdown is manifested by the renormalization-group scaling of the short-distance constants. The modified ER procedure was used to include one-pion exchange nonperturbatively in dimensional regularization with PDS. This removes the long-distance contamination from the short-distance physics and produces error plots comparable to cutoff regularization. It is not clear whether a consistent power counting with perturbative pions can be developed to also include the benefits of this nonperturbative approach.

With the understanding of what causes the EFT breakdown in model problems, we applied the modified ER techniques to the analysis of NN scattering data. Despite the clean removal of one-pion exchange effects, we found a radius of convergence of only $p \sim 300\,\mathrm{MeV}$ and unexpectedly large modified effective ranges. We were only able to reproduce this characteristic behavior using a more realistic model of nuclear forces from one-boson-exchange phenomenology. This model includes strong attractive and repulsive Yukawa potentials resulting from the exchange of scalar and vector mesons. The mass of the scalar meson, which is associated with correlated two-pion exchange, sets the breakdown scale of the EFT, and the strong coupling is the source of the large modified effective ranges. This implies that to extend the radius of convergence beyond 300 MeV, we must include correlated two-pion effects explicitly in the EFT. Since these effects are strong, a modified ER analysis could be essential.

ACKNOWLEDGMENTS

We acknowledge useful discussions with J. Gegelia, D. B. Kaplan, M. J. Savage, B. Serot, and N. Tirfessa. This work was supported in part by the National Science Foundation under Grants No. PHY–9511923 and PHY–9258270.

APPENDIX A: NUMERICAL TECHNIQUES

The two quantities needed for numerical computation of the modified ER are the Jost function $\mathcal{F}(p)$ and the derivative with respect to r of the Jost solution at the origin $f'(p,r)$. Both of these can be found by solving for the logarithmic derivative of $f(p,r)$,

$$L_p(r) = \frac{1}{f(p,r)} \frac{\partial f(p,r)}{\partial r} \ . \tag{A1}$$

By differentiating $L_p(r)$ once and using the fact that $f(p,r)$ is a solution to the Schrödinger equation, we arrive at the differential equation

$$\frac{dL_p(r)}{dr} = 2m_{\rm red}V(r) - p^2 - L_p^2(r), \qquad\qquad L_p(\infty) = ip, \tag{A2}$$

which can be solved as a coupled equation for both the real and imaginary parts of $L_p(r)$ and for $L_p(0) \equiv L_p$ in particular. The real part of L_p is needed in the modified ER function, Eq. (11), and the imaginary part can be shown to be

$$\mathrm{Im}\, L_p = \frac{p}{|\mathcal{F}(p)|^2} \ , \tag{A3}$$

which can be solved for the magnitude of the Jost function.

The phase of the Jost function is the negative of the phase shift for the potential $V(r)$. This can be found conveniently and accurately using the variable phase method

$$\delta'(r) = -\frac{2m_{\rm red}}{p}V(r)\sin^2\left[pr + \delta(r)\right] \ , \qquad\qquad \delta(0) = 0 \ , \tag{A4}$$

with the full phase shift given by $\delta = \delta(\infty)$. When numerically solving for a potential that includes a delta-shell,

$$V_\delta(r) = -\frac{\lambda}{2m_{\rm red}}\delta(r - R) \ , \tag{A5}$$

this method must be modified to take into account the discontinuity of the wavefunction derivative at the radius R,

$$\phi'(R_+) - \phi'(R_-) = -\lambda\phi(R_-) \ . \tag{A6}$$

This can be accomplished by integrating Eq. (A4) out from the origin to $r = R_-$ and then using the new value

$$\delta(R_+) = -pR + \arctan\left[\frac{t(R_-)}{1 - \frac{\lambda}{p}t(R_-)}\right] \ , \qquad t(r) \equiv \tan\left(pr + \delta(r)\right) \tag{A7}$$

to continue the integration to infinity.

APPENDIX B: GREEN'S FUNCTION IN THE PDS SCHEME

We follow Ref. [4] in solving the S-wave radial Schrödinger equation. Since the short-range potential Eq. (14) is proportional to a delta-function, we can separate it out to give

$$(H_L - E)\psi(r) = -V_S(r)\psi(r) = -V_S(r)\psi(0) \, . \tag{B1}$$

Away from the origin, the full wavefunction ψ only depends on the regular and irregular solutions of the purely long-range potential [16]:

$$\begin{aligned} \psi_R(r) &= \frac{\mathcal{F}_L(-p)}{2ipr} f_L(p,r) + \text{c.c.} \\ \psi_I(r) &= \left[\frac{1}{2\mathcal{F}_L(p)r} f_L(p,r) + \text{c.c.}\right] - B\ \psi_R(r) \ , \end{aligned} \tag{B2}$$

with B a momentum-dependent coefficient that is inconsequential to our result. These wavefunctions satisfy $(H_L - E)\psi_R = 0$ and $(H_L - E)\psi_I = (4\pi/M)\delta^3(r)$. The Green's function $G_E(r, r' = 0) = \langle 0|(E - H_L + i\epsilon)^{-1}|r\rangle$ can therefore be written as a combination of the regular and irregular solution that cancels the incoming spherical wave,

$$G_E(r,0) = -\frac{M}{4\pi}\left[\psi_I(r) + \left(B + \frac{ip}{|\mathcal{F}_L(p)|^2}\right)\psi_R(r)\right] = -\frac{M}{4\pi r}\frac{f_L(p,r)}{\mathcal{F}_L(p)} \ , \tag{B3}$$

with the last equality following from Eq. (B2).

The divergent quantity $G_E(0,0)$ can be separated into a momentum dependent term needed for the modified ER function Eq. (11) and a regularization scheme dependent constant

$$-\frac{4\pi}{M}\mathrm{Re}\, G_E^{\mathrm{reg}}(0,0) \equiv \mathrm{Re}\left[\frac{f_L'(p,0)}{\mathcal{F}_L(p)}\right]^{\mathrm{reg}} - \frac{4\pi}{M}\mathrm{Re}\, G_0^{\mathrm{reg}}(0,0) \ . \tag{B4}$$

The first term is the logarithmic derivative of the Jost solution $f_L(p,r)$ at the origin and, up to a constant, does not depend on the regularization scheme. Using the PDS scheme, the second term is [4,7]

$$-\frac{4\pi}{M}\mathrm{Re}\, G_0^{\mathrm{PDS}}(0,0) = \mu + \alpha_\pi M \ln\frac{\mu}{m_\pi} + c_\pi \ . \tag{B5}$$

Since a momentum-independent term can be shuffled between the two terms on the right-hand side of Eq. (B4), the constant c_π is arbitrary. The imaginary part of $G_E(0,0)$ can be read directly from Eq. (B3), leading to the full Green's function

$$-\frac{4\pi}{M}G_E^{\mathrm{PDS}}(0,0) = \mathrm{Re}\left[\frac{f_L'(p,0)}{\mathcal{F}_L(p)}\right]^{\mathrm{reg}} + \mu + \alpha_\pi M \ln\frac{\mu}{m_\pi} + c_\pi + \frac{ip}{|\mathcal{F}_L(p)|^2} \, , \tag{B6}$$

as used in the text.

REFERENCES

[1] S. Weinberg, Phys. Lett. **B251** (1990) 288; Nucl. Phys. **B363** (1991) 3.

[2] G. Ecker, "Pion-pion and Pion Nucleon Interactions in Chiral Perturbation Theory," hep-ph/9710560, and references therein.

[3] U. van Kolck, Ph.D. thesis, U. Texas, Aug. 1993;
C. Ordonez, L. Ray, and U. van Kolck, Phys. Rev. Lett. **72** (1994) 1982; Phys. Rev. **C53** (1996) 2086.

[4] D. B. Kaplan, M. J. Savage, and M. B. Wise, Nucl. Phys. **B478** (1996) 629.

[5] D. R. Phillips and T. D. Cohen, Phys. Lett. **B390** (1997) 7;
D. R. Phillips, S. R. Beane, and T. D. Cohen, Ann. Phys. **263** (1998) 255;
K. A. Scaldeferri, D. R. Phillips, C.-W. Kao, and T. D. Cohen, Phys. Rev. **C56** (1997) 679.

[6] K. G. Richardson, M. C. Birse, and J. A. McGovern, "Renormalization and Power Counting in Effective Field Theories for Nucleon-Nucleon Scattering," hep-ph/9708435.

[7] D. B. Kaplan, M. J. Savage, and M. B. Wise, Phys. Lett. **B424** (1998) 390; "Two-nucleon Systems from Effective Field Theory," nucl-th/9802075.

[8] G. P. Lepage, "How to Renormalize the Schrodinger Equation," nucl-th/9706029.

[9] J. Gegelia, "Chiral Perturbation Theory Approach to NN Scattering Problem," nucl-th/9802038; "Are Pions Perturbative in Effective Field Theory?" nucl-th/9806028.

[10] U. van Kolck, "Nucleon-Nucleon Interaction and Isospin Violation," hep-ph/9711222; "Effective Field Theory of Short-Range Forces," nucl-th/9808007.

[11] J. V. Steele and R. J. Furnstahl, Nucl. Phys. **A637** (1998) 46.

[12] P. F. Bedaque and U. van Kolck, Phys. Lett. **B428** (1998) 221;
P. F. Bedaque, H.–W. Hammer, and U. van Kolck, Phys. Rev. **C58** (1998) R641.

[13] T.-S. Park, K. Kubodera, D-P. Min, and M. Rho, "The Power of Effective Field Theories in Nuclei: the Deuteron, NN Scattering and Electroweak Processes," nucl-th/9807054; T.-S. Park, K. Kubodera, D-P. Min, and M. Rho, Phys. Rev. **C58** (1998) R637.

[14] H. van Haeringen and L. P. Kok, Phys. Rev. **A26** (1982) 1218.

[15] M. L. Goldberger and K. M. Watson, *Collision Theory*, (Wiley, New York, 1964).

[16] R. G. Newton, *Scattering Theory of Waves and Particles*, (Springer-Verlag, New York, 1982).

[17] A. M. Badalyan, L. P. Kok, M. I. Polikarpov, and Y. A. Simonov, Phys. Rep. **82** (1982) 31.

[18] R. Machleidt, Adv. Nucl. Phys. **19** (1989) 189.

[19] V. G. J. Stoks, R. A. M. Klomp, M. C. M. Rentmeester, and J. J. de Swart, Phys. Rev. **C48** (1993) 792.

[20] R. B. Wiringa, V. G. J. Stoks, and R. Schiavilla, Phys. Rev. **C51** (1995) 38.

[21] R. J. Furnstahl, B. D. Serot, and H.-B. Tang, Nucl. Phys. **A615** (1997) 441.